China Geology 6 (2023) 395−408

China Geology

Journal homepage: http://chinageology.cgs.cn
https://www.sciencedirect.com/journal/china-geology

Late Quaternary fluvial terrace formation in the Luan River drainage basin, north China and its possible linkages with climate change and tectonic activation

Yu-chen Tian[a], Xu-jiao Zhang[a,*], Zhi-qiang Yin[b,*], Hai Shao[b], Ming-xu Gu[c], Yingying -Ding[a], Chao Peng[a], Xiang-ge Zhang[a]

[a] *School of Earth Sciences and Resources*, *China University of Geosciences (Beijing)*, *Beijing* 100083, *China*
[b] *China institute of Geo-Environment Monitoring*, *China Geological Survey*, *Ministry of Natural Resources*, *Beijing* 100081, *China*
[c] *Hebei geological environment monitoring Institute*, *Shijiazhuang* 050021, *China*

ARTICLE INFO

Article history:
Received 20 September 2022
Received in revised form 18 November 2022
Accepted 21 November 2022
Available online 21 February 2023

Keywords:
River terrace
Paleoclimate change
Tectonic activation
Optically stimulated luminescence dating
Marine isotope stage
Last glacial maximum
Neotectonics
Geomorphology
Geological survey engineering
North China Plain

ABSTRACT

The Luan River is the most important water system in north-eastern Hebei Province, China and is located in the transitional zone of the Eastern Yan Mountains, North China Plain and Songliao Plain. The well-developed river terraces of its tributary, the Yixun River, provide excellent information for studying neotectonics and climate change. There are seven terraces in the lower reaches of the Yixun River, numbered T7–T1. The optically stimulated luminescence dating results of 23 samples show that terraces T7–T2 formed at 111.36±5.83 ka, 78.20±4.45 ka, 65.29±4.15 ka, 56.44±3.07 ka, 40.08±2.66 ka, and 13.14±0.76 ka, respectively. A comparison with the oxygen isotope curves of deep-sea sediments reveals that the sediment formation of each terrace corresponded to cold periods of marine isotope stages MIS 4 and MIS 2 and the relatively cold periods of MIS 5e, MIS 3, and MIS 1. Since the Late Pleistocene, the incision rate of the Yixun River has ranged from 0.371–1.740 mm/a. During the formation of T7–T6, T5–T4, T4–T3, and T3–T2, the incision rate was low. However, in the two stages during which T6–T5 and T2–T1 formed (13.14±0.76 ka to 0.58±0.08 ka and 10.79±0.64 ka to 0.16±0.01 ka), these rates reached 1.554 mm/a and 1.592–1.740 mm/a, respectively. At approximately 30 ka, the activity of the Langying Fault increased, leading to footwall uplift. The river gathered in the north of Langying to form the ancient Erdaowan Lake, which resulted in the drying of the river in the lower reaches of the Yixun River during the last glacial maximum without forming river deposits. In the Early Holocene, headward erosion in the lower reaches of the Yixun River was enhanced, which resulted in the disappearance of the lake, and incised meandering formed due to increased neotectonism. Based on the analyses of river incision and the formation of ancient lakes and incised meandering, it was inferred that there have been three periods of strong tectonism in the river basin since the Late Pleistocene.

1. Introduction

River terraces are an important part of fluvial landforms, which have long been attracting researchers (Chang QF et al., 2017; Singh AK et al., 2017; Olszak J and Alexanderson H, 2020; Viveen W et al., 2020; Wesnousky SG and Owen LA, 2020; Zhang JY et al., 2021). They exhibit clear responses to tectonic movement and climate change and are considered valuable records of neotectonism and climate change (Jia LY et al., 2016; Zheng GS et al., 2017; Wang JL et al., 2018; Wu HH et al., 2019; Tao YL et al., 2020). It is generally believed that the formation and development of river terraces is a mutual result of climate change and tectonic uplift, with major controlling factors varying among study areas (Kothyari GC et al., 2016; Bender AM et al., 2020). The study of river terraces can provide important information about the changes in paleoclimate and tectonic activity (Zhang JF et al., 2010; Stokes M et al., 2012; Wang YG et al., 2021), and plays a vital role in reconstructing the evolution of fluvial landforms.

The Luan River on the north-eastern North China Plain originates in Fengning County, Hebei Province, and flows

First author: *E-mail address*: yuchentian0533@163.com (Yu-chen Tian).

* Corresponding author: *E-mail address*: zhangxj@cugb.edu.cn (Xu-jiao Zhang); yinzhiqiang@mail.cgs.gov.cn (Zhi-qiang Yin).

Literary editor: Xi-jie Chen
doi:10.31035/cg2022075
2096-5192/© 2023 China Geology Editorial Office.

into Bohai Bay from Laoting County; the total length of the trunk stream is approximately 900 km (Wang WG et al., 2017; Chen X et al., 2018; Li M et al., 2019; Niu ZX et al., 2019; Lu CS et al., 2020; Yan XL et al., 2020; Sun HY et al., 2020; Yang HF et al., 2021; Chen H et al., 2022; Li M et al., 2022; Xing B et al., 2022). The middle reaches of the Luan River, which pass through Chengde in Hebei, are located in the transitional zone at the triple-junction of the Yan Mountains, the North China Plain and the Songliao Plain. The response of fluvial geomorphology in the basin to the changes in climate and tectonic activity is more sensitive than that in plain areas (Jiang Y et al., 2015; Liu M et al., 2016; Ren WN et al., 2016; Sun YL et al., 2019; Tian YL et al., 2019; Yang WT et al., 2019; Wei XF et al., 2020). In the past, research on paleoclimate in the Luan River Basin mainly focused on the upper reaches, but quantitative evidence was insufficient, and research on neotectonics was rare (Liu YH et al., 2014; Yang XL et al., 2017; Liu LJ et al., 2018; Qi HH et al., 2018; Huang SK et al., 2020). Through the evaluation of crustal stability, it has been suggested that the crust has been stable, and there have been few active faults since the Late Pleistocene in the middle reaches of the North China Plain and Songliao Plain (Qiang ZJ and Zhang LR, 1983; Liu K and Wang JM, 2005; Liu JW et al., 2014). Therefore, since the Late Pleistocene, the development of river terraces in the middle reaches (geomorphic transition zone) should have only been affected by climate changes and not by neotectonism? Therefore, the study may provide important geomorphic evidence for evaluating regional crustal stability, a reference basis for the construction and evaluation of an ecological civilization in Chengde, as well as evidence for the reconstruction of the Quaternary paleoclimate in the transitional zone.

Through a field investigation, the authors found that the lower reaches of the Yixun River, a primary tributary of the middle reaches of the Luan River, developed river terraces with relatively complete sequences, and three sections developed incised meandering after terrace 2 (T2) due to the progress of neotectonic movement. Based on a detailed field investigation and measurements of the transverse section of the river valley, the sequence of the river terraces in the Yixun River was determined, the chronosequence was established using optically stimulated luminescence (OSL) dating, and the coupling between the formation of the terraces and climate change was explored. The features and mechanisms of tectonic movement in the lower reaches of the Yixun River since the Late Pleistocene were also studied by calculating the rates of river incision, studying the incised meandering and analysing the potential reasons why no terraces were formed during the last glacial maximum (LGM). The present results provide new insights into the formation and evolution of fluvial landforms in the middle reaches of the Luan River and their relationships to climate and neotectonism.

2. Regional setting

The city of Chengde in Hebei is located at the junction of the Yan Mountains, the North China Plain, and the Songliao Plain (Wang RF et al., 2017; Wei XF et al., 2020; Tian YC et al., 2022; Yin ZQ et al., 2022). The northern part of the Luan River Basin has a temperate continental climate, whereas the southern part has a temperate monsoon climate, with a mean annual temperature of 7.6°C and a mean annual precipitation of 520 mm (Geng XJ et al., 2020; Miao YJJ et al., 2020). The Yixun River originates from Hariha Township, in Weichang County (Hebei), with a drainage area of 6689.3 km^2 and a total length of 214 km, and it meets the Luan River in the town of Luan (Wu LY et al., 2020; Sun HY et al., 2021; Fig. 1).

The study area is located in the Shuangluan District of Chengde, which primarily comprises Mesoproterozoic, Mesozoic, and Cenozoic strata. Jurassic strata are the most widely distributed and account for 65.3% of the total area. Alluvial, pluvial, and lacustrine sediments are distributed in the valley of the study area; pluvial sediments are primarily

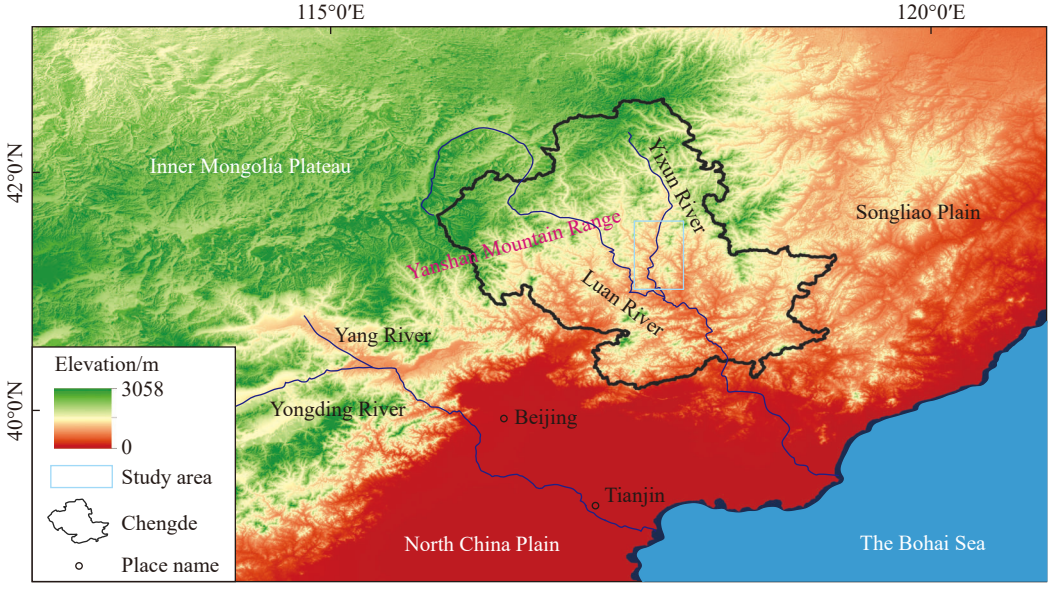

Fig. 1. Regional map of the Luan River Basin and its primary tributary, the Yixun River.

distributed in the valley of the lower reaches of the Yixun River, and lacustrine sediments are primarily distributed in the area of the ancient Erdaowan Lake in the north of Langying (Yin ZQ et al., 2020; Fig. 2). The faults are roughly NE–SW-trending in the lower reaches of the Yixun River.

3. Materials and methods

3.1. Classifying the sequence of fluvial terraces

An indoor study is helpful to improve the efficiency of fieldwork (Blaschke T et al., 2014; Wang ZH et al., 2018; Guo C et al., 2021). Based on satellite remote sensing, a digital elevation model and 1:50000-scale geological map issued by the State Geological Survey of China were combined with a detailed field investigation. This method allowed us to locate some useful river terrace profiles in the lower reaches of the Yixun River, and three representative profiles were observed, measured, and sampled. Moreover, the overall uplift of the region caused by neotectonic movement leads to the decline in the erosion base level, the further downcutting of rivers, and the formation of multi-level terraces, which are high-quality features for the study of neotectonic movement. Therefore, identification of river terraces in each section of the lower reaches of the Yixun River, analysis of characteristics of river facies sediments, and comparative study of the height above the river were carried out to explore the sequence of river terraces in the study area. During the field survey, the points of each profile and the height above the river of each terrace were accurately recorded, so as to draw a river terrace phase map of the lower reaches of the Yixun River.

3.2. Geomorphic dating (OSL dating)

River terrace sequences and chronosequences form the basis for studying the changes in paleoclimate and neotectonism of fluvial landforms (Burbank DW, 2002; Vandenberghe J et al., 2010; Junior APM et al., 2011; Guo YJ et al., 2012). Optically stimulated luminescence dating has been widely used in studying Late Pleistocene sediments (Gu JN et al., 2016; An FY et al., 2018; Cao GJ et al., 2019; Zhao XT et al., 2020; Viveen W et al., 2021). At the same time, the Loess overlying the river terrace in the study area is a high-quality dating material, which can provide a good chronological constraint for the formation of river terraces. Based on the degree of weathering of fluvial sediments in the study area, the authors preliminarily determined that the highest river terrace in the area formed during the early Late Pleistocene. Owing to its high dating range accuracy and

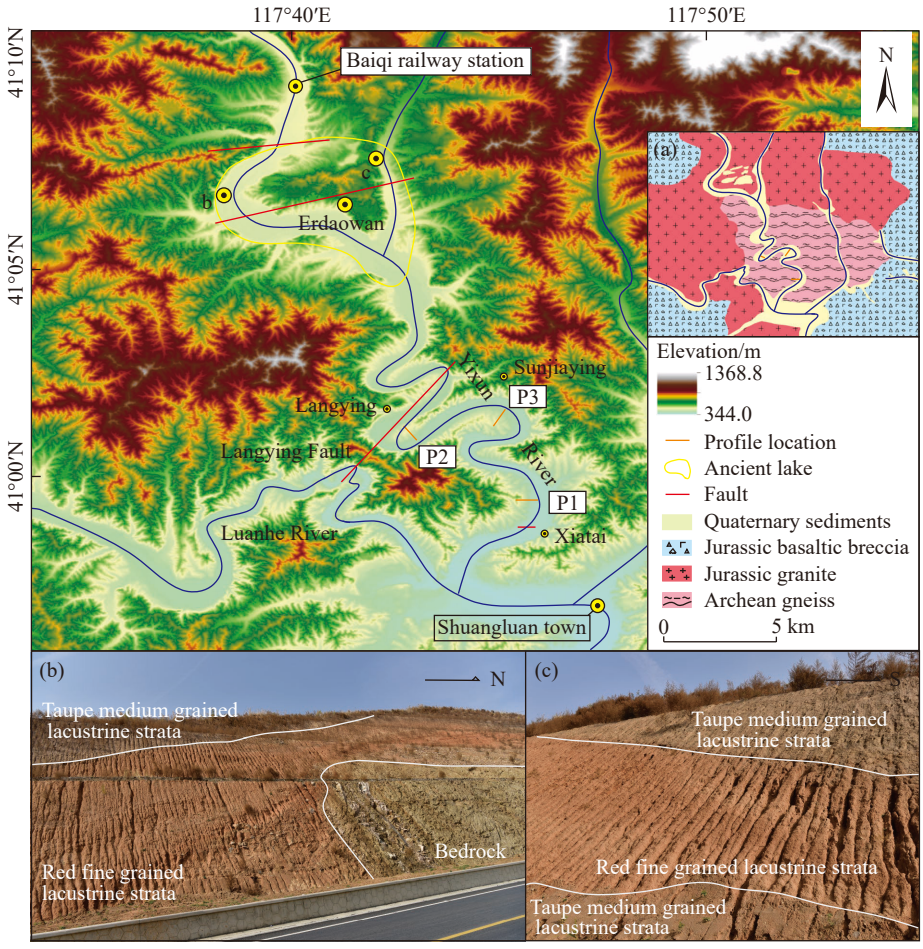

Fig. 2. Map of river terrace sections, faults, and ancient lakes in the lower reaches of the Yixun River. (a) shows the regional geology of the lower reaches of the Yixun River. (b) and (c) are the photos of paleo-lacustrine sediments in Erdaowan and are marked in the figure. Xiatai section (P1), Langying section (P2), and Sunjiaying section (P3).

consistency in previous estimates of the formation age of the terraces in the Yixun River (Zeng FM et al., 2017; He ZT et al., 2018; Wang XL et al., 2021; Wang XZ et al., 2021), OSL dating was selected as the research method.

3.2.1. Sampling

In this study, 23 OSL samples were collected, including nine samples from the Xiatai section (P1), eight samples from the Langying section (P2), and six samples from the Sunjiaying section (P3). All steel pipes with a length of 20 cm, an inner diameter of 6 cm, and one end filled with opaque material were selected for profile sampling. The contamination of samples was avoided during sampling, and a storage environment without light and where the moisture content of the sample will not change were ensured.

3.2.2. Testing

Samples were sent to the Laboratory of Earthquake Dynamics, China Earthquake Administration, for OSL testing in November 2019. After the standard pre-treatment process, the test pieces were made with silicone oil (Li ZJ et al., 2020; Nian XM et al., 2021), and subsequent analyses were carried out on automatic Risø DA-20-TL/OSL instruments (DTU Nutech, Denmark). Combined with the particle size characteristics of the OSL samples, the equivalent dose was measured using a single aliquot regeneration dating protocol (Murray AS and Wintle AG, 2000, 2003). An inductively couple plasma-mass spectrometer (NexION 300D, PerkinElmer, Inc., USA) and graphite furnace atomic absorption analyser (Z-2000, Hitachi, Ltd., Japan) were used to measure the contents of U, Th, and K, as well as the environmental dose rate via superposition and conversion of various methods (Das A et al., 2020).

3.3. Sedimentology of terrace sediments (gravel analysis)

Gravel statistics and analysis are an important part of the study of river terrace sediments. Because the characteristics of gravels of different origins differ, gravel statistics and analysis can well explore their genesis. Gravel statistics and analyses were used to determine gravel lithology, tendency, particle size, degree of weathering, and other factors to study their origin and verify the field identification of river terraces. (Miller KL et al., 2014; Jia LY et al., 2016; Li WD et al., 2020). More gravel was exposed in T2 in the Sunjiaying section, and therefore, gravel statistics were carried out in this area. The difference in elevation between the two sampled areas in this section was 6 m, and the statistical area of each part was 3 m^2 (A and B in the green frame in Fig. 7). There were 70 gravel samples in the first area and 35 in the second, and the statistical factors included triaxial lengths, occurrence, lithology, roundness, and weathering degree of gravel.

4. Results

4.1. Section profiles of the lower reaches of Yixun River terraces

Most of the river terraces are distributed along the river. Some terraces that extend far away can be found easily. Most of them are fluvial facies sediments, especially gravels with high roundness and fluvial facies sands and silts with parallel bedding. These are tectonic denudation terraces, or fault block terraces composed of faults, or landslide terraces composed of bedrock landslides, which are similar to river terraces, but they are not formed by fluvial processes. That is to say the pseudoterrace formed by non-fluvial processes does not have the above characteristics.

The terrace sediments at all levels in the three sections were primarily clayey silt, silt, and medium fine sand, with highly rounded gravel, which primarily comprised volcanic breccia, diabase, granite, and vein quartz. Enhanced neotectonism resulted in the formation of incised meandering in the three sections after T2. In the field, large height differences were found between T2 and T1 in all three sections.

According to the dating and elevation data of the terraces, up to seven terraces were identified in the lower reaches of the Yixun River. The Xiatai section (P1) includes four terraces; the Langying section (P2) includes six terraces, with T3 being eroded only; and the Sunjiaying section (P3) includes all seven terraces, although T5, T4, and T3 are buried. A strong correlation was observed among the three profiles with respect to their location, fluvial sediments.

4.1.1. Xiatai section (P1)

The Xiatai section (P1) is located south of the village of Xiatai, and the elevation of the river surface was 373 m. The authors identified four terraces in this section, among which T4 was the strath terrace, and the rest were fill terraces. Loess mostly covered the upper parts of T4 and T3. The upper part of T4 is interbedded with sand, gravel, and a small amount of silt, and the lower part is mostly grey-brown silty clay until the bedrock appears where the lithology is gneissic granite with a high degree of weathering. Silty clay is the main sediment of T3 and T2; the gravels on T3 and T2 were well sorted, highly rounded, and exhibited a complex lithology. A well-exposed section (Fig. 3) can be seen in T2, which is generally grey-yellow. Due to the large incision depth, the original sediments on T1 have been covered by proluvial sediments, and some angular and poorly sorted gravel were observed. The original gravel was excavated as local residents drilled wells. There are many crops, economic forests, and a few shrubs on T1 and the floodplain is grey-yellow silt, the vegetation roots are relatively developed, and the lower part has a gravel layer with complex gravel.

4.1.2. Langying section (P2)

The Langying section (P2) is located in the southeast of the village of Langying, and the height of the river surface is 406 m. Based on the altitude and dating results, it can be inferred that T3 has been eroded from this section. Meanwhile, T6–T2 serve as the strath terraces, and T1 is a fill terrace; bedrock is exposed along the back edge of T2. The top of T6 is red paleosol, the lower part is silty clay and silt,

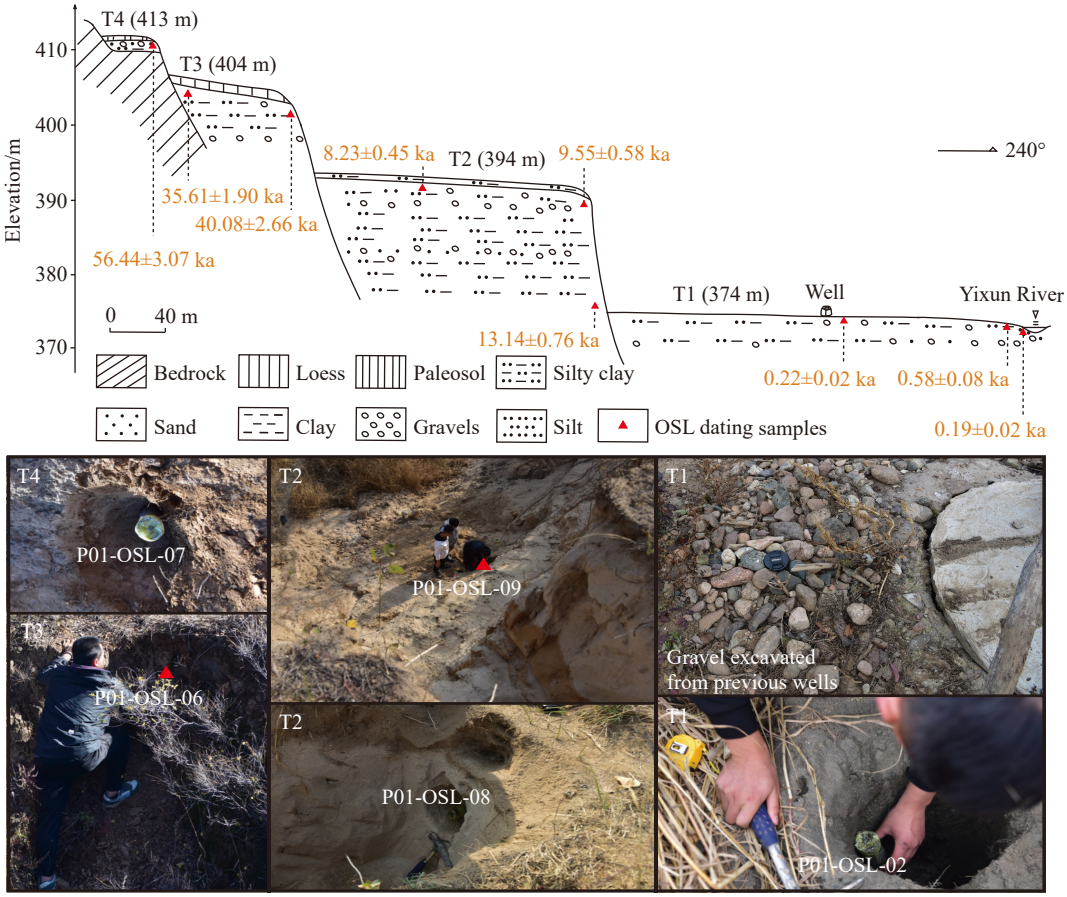

Fig. 3. Comprehensive profile of river terraces in the Xiatai section (P1), lower reaches of Yixun River.

and the bottom has a gravel layer. The fluvial sediments of T5 are silty clay, with a gravel layer and an interbedding of silty clay and sand gravel from top to bottom. The fluvial sediments of T4 and T2 are composed of silty clay, silt, and gravel. Loess was deposited at the tops of T6–T2 (Fig. 4), gravel was distributed on all levels, and abundant, well-rounded gravel could be observed on T6, T5, and T4; the main lithology is diabase, gneiss, granite, and quartz sandstone. Some poorly sorted and more angular gravel was found on T1, where many crops are planted. Based on the OSL dating of the P2-OSL-08 sample and the sedimentary characteristics (i.e., no gravel, mostly aeolian loess), it is inferred that there is a loess base below T6.

4.1.3. Sunjiaying section (P3)

The Sunjiaying section (P3) is located on the western side of the village of Sunjiaying, and the river surface is 399 m above sea level. Seven terraces were identified in this section, among which T7–T3 serve as the strath terraces, T2 and T1 are the fill terraces, and T5–T3 have been buried by the overlying loess (Fig. 5). Bedrock is exposed from T7–T3, and the degree of weathering on T7 is stronger than that on lower terraces despite the lithology being mostly gneissic granite. The lower part of the T7 taupe soil is constituted of a red paleosol and gravel layer. T6 is still dominated by a paleosol, silty clay, and gravel layer. T6 is still dominated by a paleosol, silty clay, silt, and gravel layer. There is a sand pit in T2. The south section has loess at the top, and the lower part is a red-brown paleosol composed of silty clay. The lower part of the paleosol has a gravel layer, and the lowest part has a layer of coarse sand and sand interbedded with grey to grey-yellow parallel bedding. The south section of the sand pit is integrated with the north, so the sediment characteristics are approximately the same.Fluvial gravels can be observed on T7, T6, and T2. Fluvial gravels on T7 are generally well sorted and well-rounded, and those on T6 are mostly concentrated at a depth of 3–5 cm. Many crops are planted on T5, T4, T3, and T1. Similar to the Xiatai and Langying sections, angular and poorly sorted gravels were also observed in Sunjiaying (T1). The authors speculate that the original T1 has been covered by pluvial deposits.

4.2. Gravel analysis

As mentioned above, we made gravel statistics in two areas in the Sunjiaying section. The lithologies of the gravel in the first area A primarily included volcanic hornblende, granite gneiss, metamorphic quartzite, diabase, gneiss, granite, and quartz sandstone and the lithologies of the second area B were roughly the same. Therefore, it is speculated that the sediment provenances in these two areas are similar. The degree of weathering of the gravels in these two areas was mostly weak, which corresponded with their relatively young ages. More than 42% of the gravel in area A was rounded, and

more than 45% was subrounded. The grain size in area A was small, mostly 0–15 cm (Fig. 6). Approximately 6% of the gravel in area B was well-rounded, 40% was rounded, and more than 54% was subrounded. The overall size of the gravel in area B was slightly larger than that in area A. According to the gravel analysis results, the gravel in T2 of the Sunjiaying

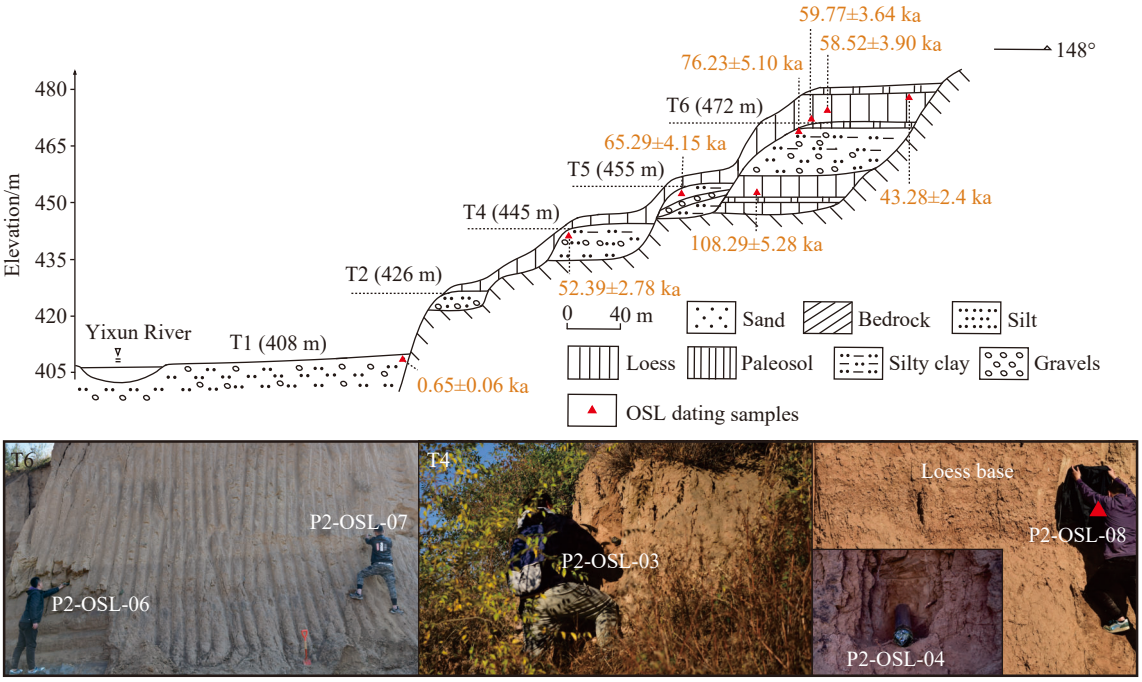

Fig. 4. Comprehensive profile of river terraces in the Langying section (P2), lower reaches of Yixun River.

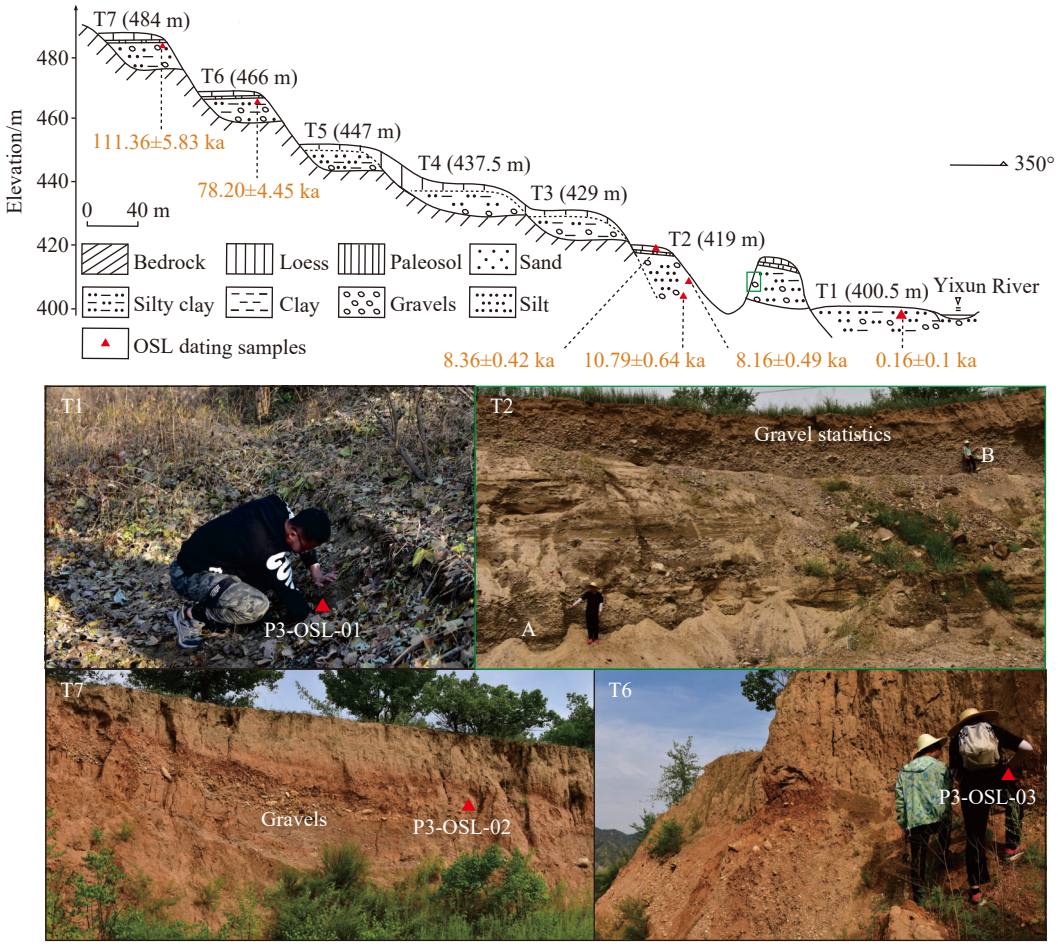

Fig. 5. Comprehensive profile of river terraces in the Sunjiaying section (P3), lower reaches of Yixun River.

section was well sorted, with a high roundness and complex petrology, indicating that it was river facies gravel. Additionally, it was further confirmed that T2 of the Sunjiaying section was a river terrace. The flat surface of the flat gravel in these two areas ranged between 180° and 270° (Fig. 7) and both were upstream. It was further confirmed that the gravel in areas A and B were fluvial facies deposits.

4.3. OSL dating results and terrace chronosequences

The data from OSL dating of the three sections were roughly consistent with the expected values (Table 1). The quartz signal in the measured data was characterized by rapid attenuation, which is a typical characteristic of this signal. The distribution of the equivalent dose in the data was relatively concentrated, indicating that the samples were fully exposed before burial and faded well. Therefore, the OSL data (Table 1) represent the time since the last exposure of the samples. Notably, although the dates of the samples obtained from all T1 sections were relatively young, the sampling and experiments followed the standard process, and the data were reliable.

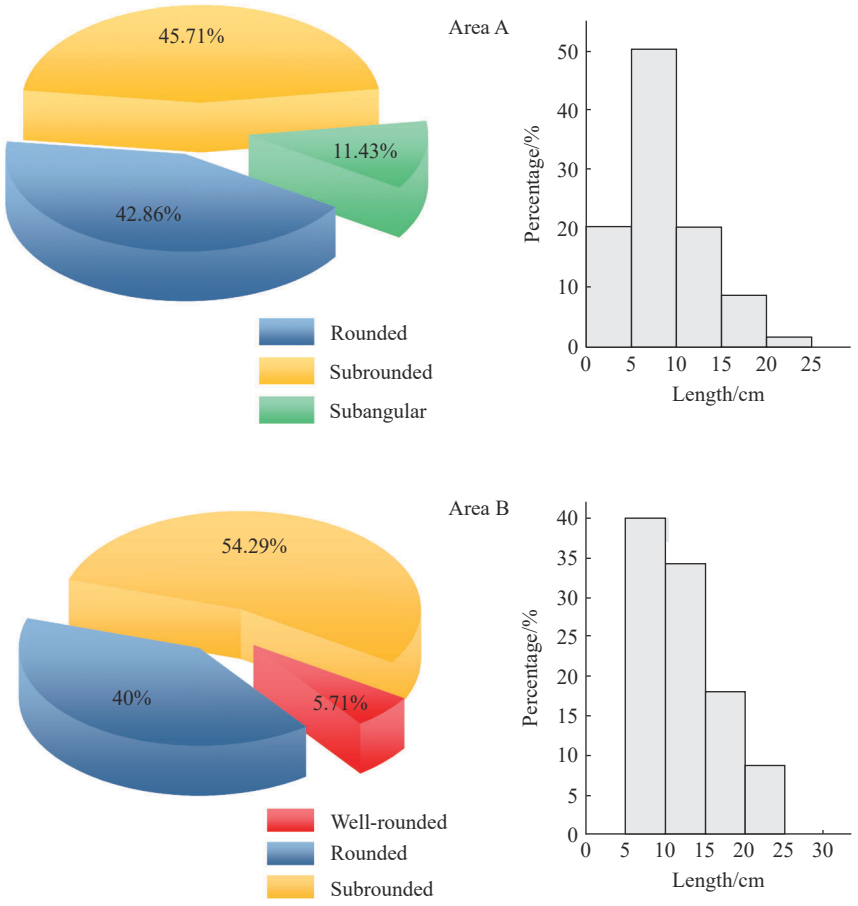

Fig. 6. Roundness and lengths of gravel in areas A and B.

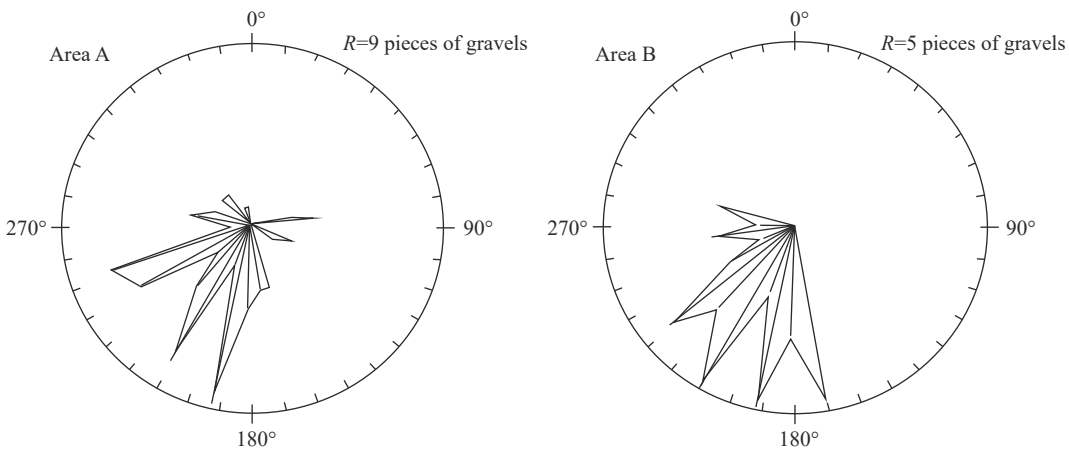

Fig. 7. Rose diagram of gravel facies slopes in areas A and B.

In this study, the oldest terrace age for all levels was set as the approximate time of terrace formation; notably, an increased neotectonism resulted in an increase in the degree of incision of the Yixun River, and three sections formed incised meandering after T2, which caused T1 sediments to be covered by pluvial sediments, resulting in a relatively young age for this terrace. The aforementioned data may indicate flood events, and therefore, only the approximate time of formation is provided. According to the dating results (Table 1) and the terrace sequence (Fig. 8, Table 2), the formation times of all terraces could be inferred; from T7 to T2, these were 111.36±5.83 ka, 78.20±4.45 ka, 65.29±4.15 ka, 52.39±2.78 ka, 40.08±2.66 ka, and 13.14±0.76 ka, respectively. The formation time of T1 was approximately during the Early Holocene.

Table 1. Results of OSL samples taken from each section.

Sample	Terrace	Dose rate/(Gy/ka)	Equivalent dose/Gy	Age/ka
P1-OSL-07	T4	2.95±0.14	166.93±4.7	56.44±3.07
P1-OSL-05	T3	3.48±0.16	139.35±6.53	40.08±2.66
P1-OSL-06	T3	3.35±0.16	119.31±3.05	35.61±1.90
P1-OSL-09	T2	2.48±0.13	32.53±0.73	13.14±0.76
P1-OSL-08	T2	2.16±0.11	20.59±0.66	9.55±0.58
P1-OSL-04	T2	2.75±0.14	22.61±0.46	8.23±0.45
P1-OSL-03	T1	3.01±0.12	0.67±0.06	0.22±0.02
P1-OSL-02	T1	3.18±0.16	1.85±0.23	0.58±0.08
P1-OSL-01	T1	2.15±0.09	0.41±0.03	0.19±0.02
P2-OSL-05	T6	3.78±0.17	287.94±14.04	76.23±5.10
P2-OSL-06	T6loess	2.99±0.13	178.47±7.62	59.77±3.64
P2-OSL-07	T6loess	3.12±0.15	182.32±8.68	58.52±3.90
P2-OSL-04	T6loess	3.16±0.14	156.73±4.36	43.28±2.4
P2-OSL-08	Loessbase	3.45±0.16	373.25±4.67	108.29±5.28
P2-OSL-02	T5	2.48±0.13	161.62±5.67	65.29±4.15
P2-OSL-03	T4	2.94±0.14	153.79±3.66	52.39±2.78
P2-OSL-01	T1	3.10±0.15	2.02±0.16	0.65±0.06
P3-OSL-02	T7	3.26±0.15	362.9±9.83	111.36±5.83
P3-OSL-03	T6	2.86±0.13	223.5±7.26	78.20±4.45
P3-OSL-04	T2	2.60±0.14	27.99±0.71	10.79±0.64
P3-OSL-06	T2loess	3.08±0.15	25.75±0.35	8.36±0.42
P3-OSL-05	T2	2.84±0.15	23.21±0.72	8.16±0.49
P3-OSL-01	T1	3.28±0.17	0.54±0.03	0.16±0.01

5. Discussion

As mentioned above, there are few previous studies and insufficient quantitative evidence on paleoclimate change and neotectonic movement in the Luan River Basin. Therefore, it remains unclear what the main factors affecting the development of river terraces in the middle reaches of Luan River in the geomorphic transition zone are, and how paleoclimate change and neotectonic movement and the

Table 2. Height above the river and ages of terraces in the three sections.

Section	Height and age	Xiatai (P1)	Langying (P2)	Sunjiaying (P3)
T1	Height above the river	2 m	2 m	1.5 m
	Age	–	–	–
T2	Height above the river	21 m	20 m	20 m
	Age	13.14 ka	–	10.79 ka
T3	Height above the river	31 m	–	30
	Age	40.08 ka	–	–
T4	Height above the river	40 m	39 m	38.5 m
	Age	56.44 ka	52.39 ka	–
T5	Height above the river	–	49 m	48 m
	Age	–	65.29 ka	–
T6	Height above the river	–	66 m	67 m
	Age	–	76.23 ka	78.2 ka
T7	Height above the river	–	–	85 m
	Age	–	–	111.36 ka

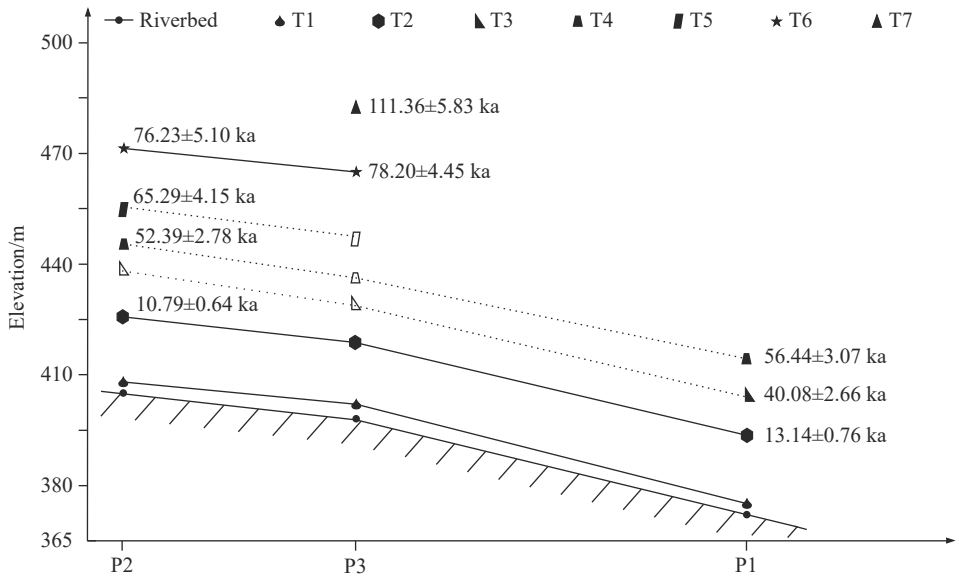

Fig. 8. Phase diagram of river terraces in the lower reaches of the Yixun River.

formation of river terraces are coupled. Thus, the authors focused on the relationship between paleoclimate change and the formation of river terraces in the study area and the possible indications for neotectonic movement.

5.1. Coupling between terrace formation and climate change since the Late Pleistocene

As mentioned above, paleoclimate change can have an important impact on the formation of river terraces. In the cold glacial period, the degree of river downcutting is weak and mostly sedimentary, while in the warm interglacial period, the ability of river downcutting is enhanced (He ZX et al., 2015; Jia LY et al., 2016). So what is the response of fluvial sediments in the lower reaches of the Yixun River to paleoclimate change? Based on the dating data of three sections and terraces at all levels, combined with the paleoclimate changes recorded by marine and Guliya ice core oxygen isotopes (Yao CD, 1999; Chen LK et al., 2011), the authors further discuss this issue in the following paragraphs.

The stages of deposition and incision of the Yixun River corresponded well with the marine oxygen isotope stages (i.e., MISs) and the oxygen isotopes of the Guliya ice core (Fig. 9). Based on the marine isotope curves, the depositional and incision processes of the river were explored. The depositional stage of T7 may be related to MIS 5d, whereas those of T6, T5, and T4 are strongly correlated with MIS 4 and MIS 3. Additionally, the sedimentation stages of T6 and T5 also corresponded well with the sixth Heinrich (H6) event, whereas that of T3 corresponded to the colder MIS 3 and the H4 event. The deposition of T2 corresponded to the stages of climate cooling in MIS 2 and MIS 1, as well as with the H1 event. Combined with the formation time of T1, the deposition of T1 corresponded to the warm to cold MIS 1. Evidently, terrace deposition at all levels did not occur in the trough of the marine oxygen isotope curve and mostly reflected cooling processes. During rises and declines in temperature after the deposition of T7, the Yixun River was roughly at equilibrium, which resulted in the failure of terrace formation in the lower reaches or to a lack of preservation

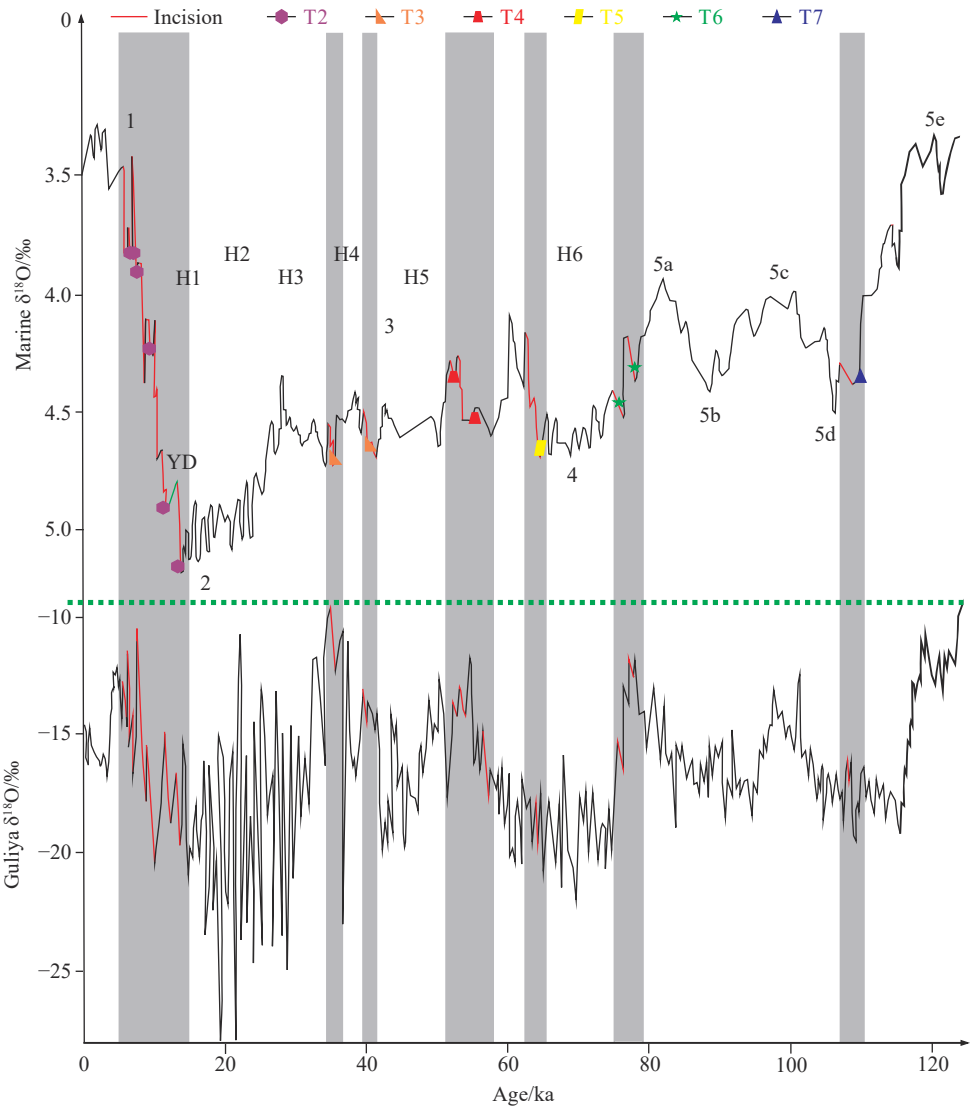

Fig. 9. Fitted curves of the formation periods of different terraces in the Yixun River with marine oxygen and oxygen isotopes of the Guliya ice core (after Shackleton NJ et al., 1983; Heinrich H, 1988; Bond GC and Lotti R, 1995; Yao CD, 1999; Chen LK et al., 2011).

during MIS 5b. The strongly incised stage of each terrace is shown in Fig. 9, and they evidently corresponded well with the warm period or warming marine isotope stages and the oxygen isotope values from the Guliya ice core. Thus, it can be concluded that the deposition of the Yixun River terraces primarily occurred during typical cold periods, such as MIS 4 and MIS 2, or during periods of sudden cooling, such as MIS 5e, MIS 3, and MIS 1. Moreover, the incision stages corresponded to hot and humid climates and warming periods.

5.2. Indications of river terraces in the lower reaches of Yixun River for neotectonic movements since the Late Pleistocene

With an advanced understanding of the relationship between river geomorphology and neotectonic movement, the indication of the river downcutting rate for neotectonic movement has been controversial in recent years. However, many scholars still believe that neotectonic movement causes the overall uplift of the region, resulting in the decline of the river erosion base level, which can accelerate river downcutting and is an important factor for accelerating river undercutting. This is an important entry point for the study of neotectonic movement (Jia LY et al., 2017), such as related to the average downcutting rate of the river terrace of the Yixun River, whether this can indicate the neotectonic movement in the study area, and whether the formation of the river terraces in the study area is affected by the neotectonic movement. Because of the close proximity and strong correlation among the three sections, the incision rate of the Yixun River was explored according to the altitude of the terraces at all levels of the three sections and their dates. Unfilled polygons in Figure 10 represent denuded or buried terraces, and T2 in the Langying section is represented by polygons with black edges (Fig. 10). Because there were multiple OSL samples distributed on T2 in sections P1 and P3, no OSL samples were taken for T2 in section P2.

The incision of the lower reaches of the Yixun River since the Late Pleistocene can be divided into the following stages: T7 was formed at about 111 ka, and the authors did not calculate the incision rates of the Yixun River during this period because the authors did not find a higher-level terrace. The average rate of river incision during the formation of T7–T6 in the Sunjiaying section was determined as about 0.543 mm/a at 111–78 ka. The average incision rate of T6–T5 in the Langying section reached about 1.554 mm/a from 76–65 ka. Based on the Langying section, the average incision rate of T5–T4 was about 0.775 mm/a from 65–52 ka. Based on the Xiatai section, the average incision rate of T4–T3 was about 0.550 mm/a from 56–40 ka. According to the data on T3–T2 in the Xiatai section, from 40–13 ka, the river was estimated to be incised at a rate of 0.371 mm/a. From T2–T1 in the Sunjiaying section, the incision rate of the Yixun River was estimated as 1.592 mm/a, whereas it was 1.740 mm/a in the Xiatai section. From these six stages, the incision of the Yixun River first increased, then declined, and then increased again. When assessing the reason why the average incision rate of the Yixun River reached 1.554 mm/a in the second stage, neotectonic movement, as one of the important factors affecting river terraces, cannot be ignored (Li XS et al., 2009; Guo XH et al., 2018; Wu DY et al., 2019; Zhang YQ et al., 2019). Additionally, the fluctuations in sea level decreased the erosion base level and increased the river incision rate (Demoulin A and Hallot E, 2009; Ishihara T et al., 2012; Bridgland DR and Westaway R, 2014; Faulkner DJ et al., 2016; Yuan Y et al., 2016). The T2–T1 incision rate of the Yixun River reached about 1.592–1.740 mm/a. The first reason for this was that enhanced neotectonism in the region after T2 formed an incised meander, which resulted in large

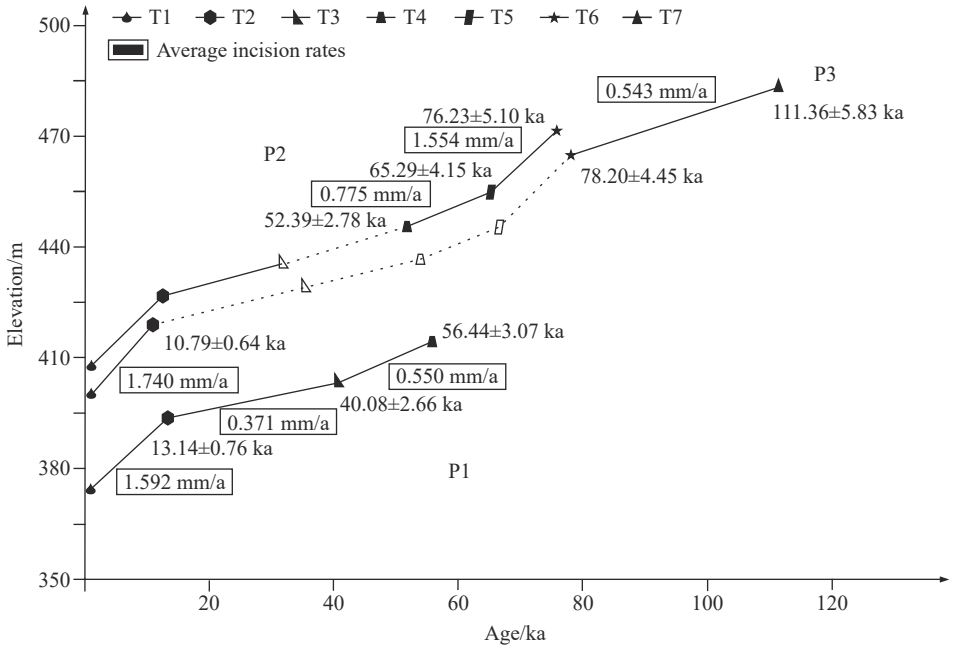

Fig. 10. Average incision rate determined by the river terraces in the lower reaches of the Yixun River (Dotted lines indicate terraces that are not exposed due to erosion or burial.).

differences in terrace height. Secondly, the Holocene temperature gradually increased, which accelerated river incision.

During the study of the river terraces in the lower reaches of the Yixun River, the authors found some characteristics of neotectonic movement. During the LGM, the temperature declined sharply; however, no river terraces were formed in the lower reaches of the Yixun River (Fig. 9). During field investigation, no deposits from the LGM were found in the three sections, and an incised meander was formed in the three sections after T2. It is inferred that there is an active fault in the north of Langying based on the dating of river terrace samples, remote sensing images, and the most important geomorphological evidence, that is, the synchronous bending of the water system. According to the lack of Last Glacial Maximum OSL samples of the terrace in the lower reaches of Yixun River, it is speculated that the activity of this fault was enhanced at about 30 ka, resulting in the formation of ancient lakes in the north. Subsequently, this caused the water in the lower reaches of the Yixun River to dry up. With climatic warming, water flow and headward erosion in the lower reaches of the Yixun River increased, the river flowed downstream, and the lake disappeared. The ancient Erdaowan Lake is preserved in the north of the Langying section (Fig. 2), which has a wide range of clearly lacustrine characteristics. These characteristics, as well as the specific time of their formation and disappearance, and the transition between fluvial and lacustrine facies warrant further exploration. Relevant progress will be reported in a subsequent study. After T2, a strong neotectonic movement occurred, which resulted in an increase in the degree of river incision and the formation of an incised meander. Therefore, the samples taken on T1 are new (P1-OSL-01, P1-OSL-02, P1-OSL-03, P2-OSL-01, and P3-OSL-01), because the three sections after T2 have been heavily incised to form an incised meander. Floods occurred in the upper reaches of the river, which caused T1 to be buried. According to the age data from these samples, the times of the two flood events were about 0.65–0.58 ka and about 0.22–0.16 ka, which may be related to the recent increase in temperature in the Luan River Basin. Combined with the sudden increase in the rate of incision during the second stage, it can be inferred that there were three periods of relatively strong neotectonism in the lower reaches of the Yixun River. The authors infer the existence of Langying Fault through the synchronous bending of the water system. This is actually the difference between neotectonic and tectonic movement. The authors discuss the change of the water system through the morphology of landforms, that is, the control and influence of an active fault on the water system. The synchronous bending of the water system is a particularly typical change. From the perspective of geomorphology, a change in a water system is controlled by an active fault. Some field investigation and dating samples are still needed to find out the activity and the characteristic of the fault, which is still meaningful. Relevant progress will be reported in a subsequent study.

5.3. Factors controlling the formation of terraces in the Yixun River

Evidently, the deposition and incision of the Yixun River were highly coupled with climate change; however, this does not mean that neotectonic movement did not influence the formation of the river terraces. As previously noted, the incision rates of the Yixun River have increased abruptly, reaching 1.554 mm/a and 1.592–1.740 mm/a, which is likely impossible if climate change alone affected the rates of the river incision. Moreover, neotectonic movement has caused the differential uplift of the lower reaches of the Yixun River, leading to the drying up of the downstream area, failure of terrace formation during the LGM, and formation of an incised meander after T2 in all three sections. Therefore, the authors believe that the formation of the terraces of the Yixun River has been mutually influenced by climate change and neotectonism.

6. Conclusions

(i) Since the Late Pleistocene, seven river terraces have developed in the lower reaches of the Yixun River, the primary tributary of the Luan River in Chengde, Hebei Province. According to OSL dating results, the formation times of T7–T2 were approximately 111.36±5.83 ka, 78.20±4.45 ka, 65.29±4.15 ka, 56.44±3.07 ka, 40.08±2.66 ka, and 13.14±0.76 ka, respectively. Because T1 was deeply incised and then covered by proluvial sediments, the authors estimated that it formed in the Early Holocene.

(ii) The formation of terraces in the Yixun River is highly consistent with the records of the Guliya ice core and marine oxygen isotope records, showing more evident responses to climate change. Their deposition mostly occurred during typical cold periods, such as MIS 4 and MIS 2, or during cooling periods, whereas incision primarily occurred during warming periods. Two flood events also occurred in the lower reaches of the Yixun River at 0.65–0.58 ka and 0.22±0.16 ka, which were mostly related to modern increases in temperature in the Luan River Basin.

(iii) Additionally, it is because of neotectonic movement that the incision rates of the Yixun River increased between 76.23±5.10 and 65.29±4.15 ka, and that no terraces were formed during the LGM. Incised meandering formed after T2, which provides evidence for the enhancement of neotectonism. The terraces in the lower reaches of the Yixun River have recorded three strong neotectonic movements in the Luan River Basin since the Late Pleistocene, and the formation of these terraces was jointly influenced by climate change and neotectonism.

CRediT authorship contribution statement

Yu-chen Tian, Xu-jiao Zhang and Zhi-qiang Yin conceived of the presented idea. Hai Shao, Ming-xu Gu, Ying-ying Ding, Chao Peng, Xiang-ge Zhang, Jun-xiang Zhao contributed to the core data preparation. All authors discussed the results and contributed to the final manuscript.

Declaration of competing interest

The authors declare no conflicts of interest.

Acknowledgments

The author thanks the reviewers and editors who participated in the manuscript review. This work was supported by the National Natural Science Foundation of China (41977258), the China Geological Survey (DD20190310, DD20221761) and the National Key R&D Program of China (2018YFC1504704).

References

An FY, Lai ZP, Liu XJ, Wang YX, Chang QF, Lu BL, Yang XY. 2018. Luminescence chronology and radiocarbon reservoir age determination of lacustrine sediments from the Heihai Lake, NE Qinghai-Tibetan Plateau and its paleoclimate implications. Journal of Earth Science, 29(3), 695–706. doi: 10.1007/s12583-017-0972-9.

Bender AM, Lease RO, Corbett LB, Bierman PR, Caffee MW, Rittenour TM. 2020. Late Cenozoic climate change paces landscape adjustments to Yukon River capture. Nature Geoscience, 13(8), 571–575. doi: 10.1038/s41561-020-0611-4.

Blaschke T, Hay GJ, Kelly M, Lang S, Hofmann P, Addink E, Feitosa RQ, Meer FCD, Werff HVD, Coillie FV, Tiede D. 2014. Geographic object-based image analysis - towards a new paradigm. Journal of Photogrammetry and Remote Sensing, 87, 180–191. doi: 10.1016/j.isprsjprs.2013.09.014.

Bond GC, Lotti R. 1995. Iceberg discharges into the North-Atlantic on millennial time scales during the Last Glaciation. Science, 267(5200), 1005–1010. doi: 10.1126/science.267.5200.1005.

Bridgland DR, Westaway R. 2014. Quaternary fluvial archives and landscape evolution: A global synthesis. Proceedings of the Geologists Association, 125(5), 600–629. doi: 10.1016/j.pgeola.2014.10.009.

Burbank DW. 2002. Rates of erosion and their implications for exhumation. Mineralogical Magazine, 66(1), 25–52. doi: 10.1180/0026461026610014.

Cao GJ, Yu L, Zhang XQ. 2019. Morphological characteristics of the paleo-channel and paleo-discharge in the middle reaches of the Yihe River in Shandong Province. Acta Geoscientica Sinica, (3), 417–427 (in Chinese with English abstract). doi: 10.3975/cagsb.2018.080802.

Chang QF, Lai ZP, An FY, Wang HL, Lei YB, Han FQ. 2017. Chronology for terraces of the Nalinggele River in the north Qinghai-Tibet Plateau and implications for salt lake resource formation in the Qaidam Basin. Quaternary International, 430, 12–20. doi: doi.org/10.1016/j.quaint.2016.02.022.

Chen H, He L, Ye SY, Han ZZ, Yuan HM, Edward AL. 2022. Differentiation of sedimentary environment and its carbon sequestration rate since the Late Pleistocene in the Luanhe River Delta, northern Bohai Bay. Geology in China, 49(5), 1555–1570 (in Chinese with English abstract). doi: 10.12029/gc20220513.

Chen LK, Lai XL, Zhao YB, Chen HX, Ni ZY. 2011. Organic carbon isotope records of paleoclimatic evolution since the Last Glacial Period in the Tangjia region, Tibet. Journal of Earth Science 22(6), 704–717. doi: 10.1007/s12583-011-0221-6.

Chen X, Li FW, Feng P. 2018. Spatiotemporal variation of hydrological drought based on the optimal standardized streamflow index in Luan River Basin, China. Natural Hazards, 91(1), 155–178. doi: 10.1007/s11069-017-3118-6.

Das A, Joseph J, Solanki T, Makwana N, Chauhan G, Thakkar MG. 2020. Reconstructing Late Quaternary Palaeo-environmental change from the dryland fluvial landscape of the Southern Kachchh Mainland, western India: Insights from new OSL and sedimentological datasets. Geological Journal, 55(10), 7041–7056. doi: 10.1002/gj.3861.

Demoulin A, Hallot E. 2009. Shape and amount of the Quaternary uplift of the western Rhenish shield and the Ardennes (western Europe). Tectonophysics, 474(3), 696–708. doi: 10.1016/j.tecto.2009.05.015.

Faulkner DJ, Larson PH, Jol HM, Running GL, Loope HM, Goble RJ. 2016. Autogenic incision and terrace formation resulting from abrupt late-glacial base-level fall, lower Chippewa River, Wisconsin, USA. Geomorphology, 266, 75–95. doi: 10.1016/j.geomorph.2016.04.016.

Geng XJ, Zhou XC, Yin GD, Hao FH, Zhang X, Hao ZC, Singh VP, Fu YH. 2020. Extended growing season reduced river runoff in Luan River basin. Journal of Hydrology, 582, 124538. doi: 10.1016/j.jhydrol.2019.124538.

Gu JN, Chen AD, Zhao ZZ, Yao HT, Li ZM, Zhang Q. 2016. Quaternary glacial deposits features and its OSL dating in mt. cangshan global geopark of Dali, Yunnan Province. Acta Geoscientica Sinica, (6), 769–778 (in Chinese with English abstract). doi: 10.3975/cagsb.2016.06.12.

Guo C, Xu Q, Dong XJ, LiWL, Zhao KY, Lu HY, Ju YZ. 2021. Geohazard recognition and inventory mapping using airborne LiDAR Data in complex mountainous areas. Journal of Earth Science, 2021,32(5), 1079–1091. doi: 10.1007/s12583-021-1467-2.

Guo XH, Forman SL, Marin L, Li XL. 2018. Assessing tectonic and climatic controls for Late Quaternary fluvial terraces in Guide, Jianzha, and Xunhua Basins along the Yellow River on the northeastern Tibetan Plateau. Quaternary Science Reviews, 195, 109–121. doi: 10.1016/j.quascirev.2018.07.005.

Guo YJ, Zhang JF, Qiu WL, Hu G, Zhuang MG, Zhou LP. 2012. Luminescence dating of the Yellow River terraces in the Hukou area, China. Quaternary Geochronology, 10, 129–135. doi: 10.1016/j.quageo.2012.03.002.

He ZT, Ma BQ, Long JY, Wang JY, Zhang H. 2018. New progress in paleoearthquake studies of the East Sertengshan piedmont fault, Inner Mongolia, China. Journal of Earth Science, 29(2), 441–451. doi: 10.1007/s12583-017-0937-z.

He ZX, Zhang XJ, Bao SY, Qiao YS, Sheng YY, Liu XT, He XL, Yang XC, Zhao JX, Liu R, Lu CY. 2015. Multiple climatic cycles imprinted on regional uplift-controlled fluvial terraces in the lower Yalong River and Anning River, SE Tibetan Plateau. Geomorphology, 250, 95–112. doi: 10.1016/j.geomorph.2015.08.010.

Heinrich H. 1988. Origin and consequences of cyclic ice rafting in the Northeast Atlantic Ocean during the past 130, 000 years. Quaternary Research, 29(2), 142–152. doi: 10.1016/0033-5894(88)90057-9.

Huang SK, Jia HJ, Wu JY, Zhang H, Yin ZQ. 2020. Environment changes revealed by grain size from Yudaokou in Bashang area since 8000 a BP. Hydrogeology and Engineering Geology, 47(6), 74–80 (in Chinese with English abstract). doi: 10.16030/j.cnki.issn.1000-3665.202008062.

Ishihara T, Sugai T, Hachinohe S. 2012. Fluvial response to sea-level changes since the latest Pleistocene in the near-coastal lowland, central Kanto Plain, Japan. Geomorphology, 147–148, 49–60. doi: 10.1016/j.geomorph.2011.08.022.

Jia LY, Hu DG, Wu HH, Zhao XT, Chang PY, You BJ, Zhang M, Wang CQ, Ye MG, Wu ZQ, Liang XZ. 2017. Yellow River terrace sequences of the Gonghe-Guide section in the northeastern Qinghai-Tibet: Implications for plateau uplift. Geomorphology, 295, 323–336. doi: 10.1016/j.geomorph.2017.06.007.

Jia LY, Zhang XJ, Ye PS, Zhao XT, He ZX, He XL, Zhou QS, Li J, Ye MN, Wang Z, Meng J. 2016. Development of the alluvial and lacustrine terraces on the northern margin of the Hetao Basin, Inner Mongolia, China: Implications for the evolution of the Yellow River in the Hetao area since the late Pleistocene. Geomorphology, 263, 87–98. doi: 10.1016/j.geomorph.2016.03.034.

Jiang Y, Liu CM, Li XY. 2015. Hydrological impacts of climate change simulated by HIMS Models in the Luan River Basin, North China. Water Resources Management, 29(4), 1365–1384. doi: 10.1007/s11269-014-0881-y.

Junior APM, Cherem LFS, Barros LFDP, Santos GBD. 2011. OSL dating of sediments from a mountainous river in southeastern Brazil: Late Cenozoic tectonic and climatic implications. Geomorphology, 132(3), 187–194. doi: 10.1016/j.geomorph.2011.05.008.

Kothyari GC, Shukla AD, Juyal N. 2016. Reconstruction of Late Quaternary climate and seismicity using fluvial landforms in Pindar

River valley, Central Himalaya, Uttarakhand, India. Quaternary International, 443, 248–264. doi: 10.1016/j.quaint.2016.06.001.

Li M, Xu QM, Cheng LY, Yang N, Liu JB, Guo JJ. 2022. Mid-Late Holocene sedimentary evolution process in the Qilihai area, northern Luanhe Estuary. Geological Bulletin of China, 41(2-3), 242–252 (in Chinese with English abstract). doi: 10.12097/j.issn.1671-2552.2022.2-3.004.

Li M, Zhang T, Feng P. 2019. A nonstationary runoff frequency analysis for future climate change and its uncertainties. Hydrological Processes, 33(21), 2759–2771. doi: 10.1002/hyp.13526.

Li WD, Zhao XT, Yang Y, Wu ZH. 2020. Formation age and provenance analysis of the gravel layer in the Yellow River terraces of the Hetao Basin. Acta Geoscientica Sinica, (4), 515–524 (in Chinese with English abstract). doi: 10.3975/cagsb.2020.031801.

Li XS, Liu BH, Hua QF, Zhao YX, Liu CG. 2009. Characters of the Zhangj iakou-Penglai Fault Zone Activity in the Bohai Sea Since Late Quaternary. Advances In Marine Science, 27(3), 332–341 (in Chinese with English abstract). doi: 10.1016/S1874-8651(10)60080-4.

Li ZJ, Mou XS, Fan YX, Zhang QS, Yang GL, Zhao H. 2020. Establishing a common standardised growth curve for single-aliquot OSL dating of quartz from sediments in the Jilantai area of North China. Geochronometria, 47(1), 71–92. doi: 10.2478/geochr-2020-0017.

Liu JW, Wang ZM, Xie FR, Lv YJ. 2014. Seismic hazard and risk assessments in North China based on the historical intensity observations. China Earthquake Engineering Journal, 36(1), 134–143 (in Chinese with English abstract). doi: 10.3969/j.issn.1000-0844.2014.01.0134.

Liu K, Wang JM. 2005. Ground fissures and its distribution in Hebei Plain. South-to-North Water Transfers and Water Science and Technology, 3(6), 38–42 (in Chinese with English abstract). doi: 10.3969/j.issn.1672-1683.2005.06.012.

Liu LJ, Li CA, Jie DM, Zhang RC, Wang JY, Zhang YF, Mao X, Jiang GL, Wang PL. 2018. Paleoclimate recorded by phytolith in Anguli-Nuur Lake since Mid-Late Holocene. Earth Science, 43(11), 4138–4148 (in Chinese with English abstract). doi: 10.3799/dqkx.2018.614.

Liu M, Fan DJ, Liao YJ, Chen B, Yang ZS. 2016. Heavy metals in surficial sediments of the central Bohai Sea: Their distribution, speciation and sources. Acta Oceanologica Sinica, 35(9), 98–110. doi: 10.1007/s13131-016-0926-6.

Liu YH, Tian Y, Liu AR, Yang QH, Yang ZJ, Zhou YH, Guo ZX, Sun LM. 2014. Variation of Paleovegetation and Paleoclimate since the Mid-Holocene in the Yudaokou Area of Weichang County, Hebei Province. South-to-North Water Transfers and Water Science and Technology, 12(1), 69–72 (in Chinese with English abstract). doi: 10.3724/SP.J.1201.2014.01069.

Lu CS, Liu WB, Li ZM, Wu X, Kang W, Ren YX. 2020. Hydrochemical environment in a typical conservation area in the Beijing-Tianjin-Hebei region: A case study in Xinglong County of Chengde. Hydrogeology and Engineering Geology, 47(6), 132–141 (in Chinese with English abstract). doi: 10.16030/j.cnki.issn.1000-3665.202005035.

Miao YJJ, Li JZ, Feng P, Dong LX, Zhang T, Wu JZ, Katwal R. 2020. Effects of land use changes on the ecological operation of the Panjiakou-Daheiting Reservoir system, China. Ecological Engineering, 152, 105851. doi: 10.1016/j.ecoleng.2020.105851.

Miller KL, Szabó T, Jerolmack DJ, Domokos G. 2014. Quantifying the significance of abrasion and selective transport for downstream fluvial grain size evolution. Journal of Geophysical Research:Earth Surface, 119(11), 2412–2429. doi: 10.1002/2014JF003156.

Murray AS, Wintle AG. 2000. Luminescence dating of quartz using an improved single-aliquot regenerative-dose protocol. Radiation Measurements, 32(1), 57–73. doi: 10.1016/S1350-4487(99)00253-X.

Murray AS, Wintle AG. 2003. The single aliquot regenerative dose protocol: Potential for improvements in reliability. Radiation Measurements, 37(4), 377–381. doi: 10.1016/S1350-4487(03)00053-2.

Nian XM, Zhang WG, Wang ZH, Sun QL, Chen ZY. 2021. Inter-comparison of optically stimulated luminescence (OSL) ages between different fractions of Holocene deposits from the Yangtze delta and its environmental implications. Marine Geology, 432, 106401. doi: 10.1016/j.margeo.2020.106401.

Niu ZX, Jiang XW, Hu YZ. 2019. Characteristics and causes of hydrochemical evolution of deep groundwater in the Luanhe Delta. Hydrogeology and Engineering Geology, 46(1), 27–34 (in Chinese with English abstract). doi: 10.16030/j.cnki.issn.1000-3665.2019.01.04.

Olszak J, Alexanderson H. 2020. Post-IR IRSL dating the oldest (?) river terrace sediments in the Polish Outer Carpathians: Insights into the landscape evolution Geomorphology, 371, 107436. doi: 10.1016/j.geomorph.2020.107436.

Qi HH, Liu XQ, Li HS, Li JF, Cao XY, Herzschuh U. 2018. The vegetation and climate changes since the late glacial period inferred from pollen record of a sediment core in Anguli-Nuur Lake, Hebei Province. Quaternary Sciences, 38(5), 1203–1210 (in Chinese with English abstract). doi: 10.11928/j.issn.1001-7410.2018.05.14.

Qiang ZJ, Zhang LR. 1983. Regionalization of Quaternary active fractures and seismicity in China. Acta Geological Sinica, (4), 358–368 (in Chinese with English abstract).

Ren WN, Wang YX, Li JZ, Feng P, Smith RJ. 2016. Drought forecasting in Luan River basin involving climatic indices. Theoretical and Applied Climatology, 130, 1133–1148. doi: 10.1007/s00704-016-1952-1.

Shackleton NJ, Imbrie J, Hall MA. 1983. Oxygen and carbon isotope record of East Pacific core V19-30: Implications for the formation of deep water in the late Pleistocene North Atlantic. Earth and Planetary ence Letters, 65(2), 233–244. doi: 10.1016/0012-821X(83)90162-0.

Singh AK, Pattanaik JK, Jaiswal MK. 2017. Late Quaternary evolution of Tista River terraces in Darjeeling-Sikkim-Tibet wedge: Implications to climate and tectonics. Quaternary International, 443, 132–142. doi: 10.1016/j.quaint.2016.10.004.

Stokes M, Cunha PP, Martins AA. 2012. Techniques for analysing Late Cenozoic river terrace sequences. Geomorphology, 165–166, 1–6. doi: 10.1016/j.geomorph.2012.03.022.

Sun HY, Wei XF, Gan FW, Wang Heng, Jia FC, He ZX, Li DJ, Li Jian, Zhang Jing. 2020. Genetic type and formation mechanism of strontium-rich groundwater in the upper and middle reaches of Luanhe River Basin. Acta Geoscientica Sinica, 41(1), 65–79 (in Chinese with English abstract). doi: 10.3975/cagsb.2019.061701.

Sun HY, Wei XF, Jia FC, He ZX, Sun XM. 2021. Geochemical baseline and ecological risk accumulation effect of soil heavy metals in the small-scale drainage catchment of V-Ti-magnetite in the Yixun River basin, Chengde. Acta Geologica Sinica, 95(2), 588–604 (in Chinese with English abstract). doi: 10.19762/j.cnki.dizhixuebao.2020191.

Sun YL, Shan M, Pei XR, Zhang XK, Yang YL. 2019. Assessment of the impacts of climate change and human activities on vegetation cover change in the Haihe River basin, China. Physics and Chemistry of the Earth, 115, 102834. doi: 10.1016/j.pce.2019.102834.

Tao YL, Xiong JG, Zhang HP, Chang H, Li LY. 2020. Climate-driven formation of fluvial terraces across the Tibetan Plateau since 200 ka: A review. Quaternary Science Reviews, 237, 106303. doi: 10.1016/j.quascirev.2020.106303.

Tian YC, Yin ZQ, Zhang XJ, Shao H, GuM X, RenW, PengC. 2022. Sediment characteristics and paleoenvironmental significance of river terraces in the lower reaches of the Yixun River in the Yanshan Mountains. Geological Review, 68(1), 111–121 (in Chinese with English abstract). doi: 10.16509/j.georeview.2021.12.035.

Tian YL, Jiang Y, Liu Q, Dong MY, Xu DX, Liu Y, Xu X. 2019. Using a water quality index to assess the water quality of the upper and middle streams of the Luan River, northern China. Science of The Total Environment, 667, 142–151. doi: 10.1016/j.scitotenv.2019.02.356.

Vandenberghe J, Cordier S, Bridgland DR. 2010. Extrinsic and intrinsic forcing of fluvial development: Understanding natural and anthropogenic influences. Proceedings of the Geologists Association, 121(2), 107–112. doi: 10.1016/j.pgeola.2010.05.002.

Viveen W, Baby P, Sanjurjo-Sanchez J, Hurtado-Enríquez C. 2020. Fluvial terraces as quantitative markers of late Quaternary detachment folding and creeping thrust faulting in the Peruvian Huallaga basin. Geomorphology, 367, 107315. doi: 10.1016/j.geomorph.2020.107315.

Viveen W, Sanjurjo-Sanchez J, Baby P, González-Moradasad MDR. 2021. An assessment of competing factors for fluvial incision: An

example of the Late Quaternary exorheic Moyobamba basin, Peruvian Subandes. Global and Planetary Change, 200, 103476. doi: 10.1016/j.gloplacha.2021.103476.

Wang JL, Wu ZH, Zhang KQ, Sun YJ, Zhou Y. 2018. Formation age and its tectonic geomorphological significance of Qingyiji-ang River terraces in the southern of Longmenshan, Sichuan. Geological Bulletin of China, 37(6), 996–1005 (in Chinese with English abstract).

Wang RF, Zhai YL, Yu J, Liu HL. 2017. The quantitative research of mine geology environmental evaluation of Wulie River basin in Chengde. The Chinese Journal of Geological Hazard and Control, 28(2), 124–130 (in Chinese with English abstract). doi: 10.16031/j.cnki.issn.1003-8035.2017.02.17.

Wang WG, Li CN, Xing WQ, Fu JY. 2017. Projecting the potential evapotranspiration by coupling different formulations and input data reliabilities: The possible uncertainty source for climate change impacts on hydrological regime. Journal of Hydrology, 555, 298–313. doi: 10.1016/j.jhydrol.2017.10.023.

Wang XL, Peng J, Adamiec G. 2021. Extending the age limit of quartz OSL dating of Chinese loess using a new multiple-aliquot regenerative-dose (MAR) protocol with carefully selected preheat conditions. Quaternary Geochronology, 62, 101144. doi: 10.1016/j.quageo.2020.101144.

Wang XZ, Chun X, Zhou HJ, Zhang YY, Wan ZQ, Dan D. 2021. Application of standardised growth curves in quartz OSL dating of lacustrine sediments on the Mongolian Plateau. Quaternary International, 592, 51–59. doi: 10.1016/j.quaint.2021.04.018.

Wang YG, Chang H, Zhou WJ. 2021. Fluvial terrace evolution and its tectonic-climatic significance in the Weihe Basin. Geological Review, 67(4), 1033–1049 (in Chinese with English abstract). doi: 10.16509/j.georeview.2021.04.305.

Wang ZH, Lin WL, Ding RX. 2018. Quantitative Measurement of Bedding Orientation Using Remote Sensing Data: Yili Basin, Northwest China. Journal of Earth Science, 29(3), 689–694. doi: 10.1007/s12583-017-0943-1.

Wei XF, Sun HY, Zhang J, Li X, Fan LY, He ZX. 2020. Eco-geochemical process of characteristic forest fruit resources and its significance of quality improvement in Chengde City. Hydrogeology and Engineering Geology, 47(6), 99–108 (in Chinese with English abstract). doi: 10.16030/j.cnki.issn.1000-3665.202008028.

Wei XF, Wang JB, Sun HY, Yin ZQ, He ZQ, Jia FC, Li X, Liu HW, Zhang J. 2020. Exploration of land use optimization path based on geological formation in Chengde City. Hydrogeology and Engineering Geology, 47(6), 15–25 (in Chinese with English abstract). doi: 10.16030/j.cnki.issn.1000-3665.202008029.

Wesnousky SG, Owen LA. 2020. Development of the Truckee River terraces on the northeastern flank of the Sierra Nevada. Geomorphology, 370, 107399. doi: 10.1016/j.geomorph.2020.107399.

Wu DY, Li BJ, Lu HH, Zhao JX, Zheng XM, Li YL. 2019. Spatial variations of river incision rate in the northern Chinese Tian Shan range derived from late Quaternary fluvial terraces. Global and Planetary Change, 185, 103082. doi: 10.1016/j.gloplacha.2019.103082.

Wu HH, Wu XW, Li Y, Hu DG, Jia LY, Yan JD, Wang CQ, Xia MM. 2019. River terraces in the Gonghe-Guide section of the Yellow River: Implications for the late uplift of the northeastern margin of the Qinghai-Tibet Plateau. Acta Geologica Sinica, 93(12), 3239–3248 (in Chinese with English abstract). doi: 10.19762/j.cnki.dizhixuebao.2019177.

Wu LY, Zhang X, Li C, Hao FH. 2020. Impacts of climate change and human activities on runoff variations in Yixun River Basin. Journal of Natural Resources, 35(7), 1744–1756 (in Chinese with English abstract). doi: 10.31497/zrzyxb.20200717.

Xing B, Jin AF, Yin ZQ, Yin XL, Zhu WW, Wang RF. 2022. Research of basin water balance and water conservation variation based on multi-source data: A case study of Xiaoluan River Basin in Bashang plateau. Geological Bulletin of China, 41(12), 2114–2124 (in Chinese with English abstract). doi: 10.12097/j.issn.1671-2552.2022.12.004.

Yan XL, Bao ZX, Zhang JY, Wang GQ, He RM, Liu CS. 2020. Quantifying contributions of climate change and local human activities to runoff decline in the upper reaches of the Luan River basin. Journal of Hydro-environment Research, 28, 67–74. doi: 10.1016/j.jher.2018.11.002.

Yang HF, Cao WG, Zhi CS, Li ZY, Bao XL, Ren Y, Liu FT, Fan CL, Wang SF, Wang YB. 2021. Evolution of groundwater level in the North China Plain in the past 40 years and suggestions on its overexploitation treatment. Geology in China, 48(4), 1142–1155 (in Chinese with English abstract). doi: 10.12029/gc20210411.

Yang WT, Long D, Bai P. 2019. Impacts of future land cover and climate changes on runoff in the mostly afforested river basin in North China. Journal of Hydrology, 570, 201–219. doi: 10.1016/j.jhydrol.2018.12.055.

Yang XL, Zhang RC, Zhang Z, Liu LJ, Wang RJ, Gao SP. 2017. Environmental change since 5000cal. a B. P. in the Anguli-Nuur Lake area based on palynological and geochemical records. Quaternary Sciences, 37(1), 130–142 (in Chinese with English abstract). doi: 10.11928/j.issn.1001-7410.2017.01.12.

Yao CD. 1999. Abrupt climatic changes on the Tibetan Plateau during the Last Ice Age———Comparative study of the Guliya ice core with the Greenland GRIP ice core. Science in China (Series D:Earth Sciences), 42(4), 358–368. doi: 10.3321/j.issn:1006-9267.1999.02.010.

Yin ZQ, Hao AB, Wu AM, Ren JW, Zhou P, Wei XF, Peng L, Li X, Shao H, Pang JM. 2022. The key progress in Chengde and the national proposal of the integrated survey of natural resources. Geological Bulletin of China, 41(12), 2087–2096 (in Chinese with English abstract). doi: 10.12097/j.issn.1671-2552.2022.12.001.

Yin ZQ, Qin XG, Zhang JB, Wei XF, Hou HX, He ZX, Lu M. 2020. Preliminary study on classification and investigation of surface substrate. Hydrogeology and Engineering Geology, 47(6), 8–14 (in Chinese with English abstract). doi: 10.16030/j.cnki.issn.1000-3665.202010065.

Yuan Y, Kusky TM, Rajendran S. 2016. Tertiary and Quaternary Marine Terraces and Planation Surfaces of Northern Oman: Interaction of Flexural Bulge Migration Associated with the Arabian-Eurasian Collision and Eustatic Sea Level Changes. Journal of Earth Science, 27(6), 955–970. doi: 10.1007/s12583-015-0656-2.

Zeng FM, Xiang SY. 2017. Geochronology and Mineral Composition of the Pleistocene Sediments in Xitaijinair Salt Lake Region, Qaidam Basin: Preliminary Results. Journal of Earth Science, 28(4), 622–627. doi: 10.1007/s12583-016-0712-6.

Zhang JF, Qiu WL, Wang XQ, Hu G, Li RQ, Zhou LP. 2010. Optical dating of a hyperconcentrated flow deposit on a Yellow River terrace in Hukou, Shaanxi, China. Quaternary Geochronology, 5(2), 194–199. doi: 10.1016/j.quageo.2009.05.001.

Zhang JY, Yang HL, Jing LZ, Ge Yk, Wang W, Yao WQ, Xu S. 2021. Reconstructing the incision of the Lancang River (Upper Mekong) in southeastern Tibet below its prominent knickzone using fluvial terraces and transient tributary profiles. Geomorphology, 376, 107551. doi: 10.1016/j.geomorph.2020.107551.

Zhang YQ, Shi W, Dong S W. 2019. Neotectonics of North China: Interplay between far-field effect of India-Eurasia collision and Pacific subduction related deep-seated mantle upwelling. Acta Geologica Sinica, 93(5), 971–1001 (in Chinese with English abstract). doi: 10.3969/j.issn.0001-5717.2019.05.001.

Zhao XT, Jia LY, Hu DG, Li WD, Lin X, Zhang YL, Yang Y. 2020. The discovery of the Pliocene Yellow River paleochannel between Gonghe and Guide Basins, Qinghai Province: Concurrent discussion on the formation of the Longyang Gorge and the 'Gonghe Movement'. Acta Geoscientica Sinica, (4), 453–468 (in Chinese with English abstract). doi: 10.3975/cagsb.2020.070601.

Zheng GS, Xu JX, Lü JB, Luan YB, Wang JM, Yu CL, Zhang Lei. 2017. Terrace development characteristics of Dashi River valley in Western Hills of Beijing. Geological Bulletin of China, 36(7), 1251–1258 (in Chinese with English abstract).